

## Spin Field Effect Transistors with Ultracold Atoms

J. Y. Vaishnav,<sup>1</sup> Julius Ruseckas,<sup>2</sup> Charles W. Clark,<sup>1</sup> and Gediminas Juzeliūnas<sup>2</sup>

<sup>1</sup>*Joint Quantum Institute, National Institute of Standards and Technology, Gaithersburg, Maryland 20899, USA*

<sup>2</sup>*Institute of Theoretical Physics and Astronomy of Vilnius University, A. Goštauto 12, Vilnius 01108, Lithuania*

(Received 9 September 2008; revised manuscript received 20 October 2008; published 29 December 2008; corrected 14 September 2009)

We propose a method of constructing cold atom analogs of the spintronic device known as the Datta-Das transistor (DDT), which, despite its seminal conceptual role in spintronics, has never been successfully realized with electrons. We propose two alternative schemes for an atomic DDT, both of which are based on the experimental setup for tripod stimulated Raman adiabatic passage. Both setups involve atomic beams incident on a series of laser fields mimicking the relativistic spin-orbit coupling for electrons that is the operating mechanism of the DDT.

DOI: 10.1103/PhysRevLett.101.265302

PACS numbers: 67.85.-d, 37.10.Jk, 37.10.Vz, 85.75.Hh

The emerging technology of semiconductor spintronics exploits the electron's spin degree of freedom, as well as its charge state. The first scheme for a semiconductor spintronic device was a spin field-effect transistor known as the Datta-Das transistor (DDT) [Fig. 1(a)] [1]. The 18 years since the theoretical proposal have seen numerous experimental efforts to construct the DDT. Various experimental obstacles, such as difficulties in spin injection, stray electric fields, and insufficient quality of spin-orbit coupling have prevented successful implementation of the DDT [2].

Cold atom systems, in contrast with their electronic counterparts, are highly controllable and tunable. This suggests the possibility of designing precise atomic analogs of electronic systems which, due either to fundamental physical limits or technological difficulties, are experimentally inaccessible in their original manifestations. The idea grows out of recent interest in "atomtronics," or building cold atom analogs of ordinary electronic materials, devices, and circuits [3–5]. In particular, an atom diode has been proposed [3] and realized [5].

In this Letter, we identify a method for constructing a cold atom analog of a Datta-Das transistor. The setup is based on a four level "tripod" scheme of atom-light coupling [6–8] involving three atomic ground states and one excited state [see Fig. 1(b)]. Such tripod schemes are an extension of the usual three-level  $\Lambda$ -type setup for stimulated Raman adiabatic passage (STIRAP) [3,9], and are experimentally accessible in metastable Ne, <sup>87</sup>Rb and a number of other gases [10,11]. The proposed device provides a robust method for atomic state manipulation that is immune to the inhomogeneities intrinsic to programmed Rabi pulses.

The source terminal of an electronic DDT [Fig. 1(a)] is a ferromagnetic electrode that emits spin-polarized electrons. The DDT drain terminal, a ferromagnetic analyzer, acts as a spin filter. Between source and drain is a semiconducting gate region, in which the gate-induced electric field produces a Rashba spin-orbit coupling [12] for electrons. While passing through the gate region, the electron's

spin precesses; the electron emerges at the drain having undergone a spin rotation which is tunable via the gate voltage. Since the drain passes only a certain spin direction, the drain current is an oscillating function of the gate voltage.

Our atomic analog of the DDT [Figs. 1(c) and 1(d)] uses a beam of atoms in place of electrons. The two dark states in the tripod setup play the role of the electron's spin states, and the "source" is a dilute atomic beam. The "gate" region consists of crossed laser beams engineered to mimic Rashba or Rashba-like spin-orbit couplings [13–17]; the

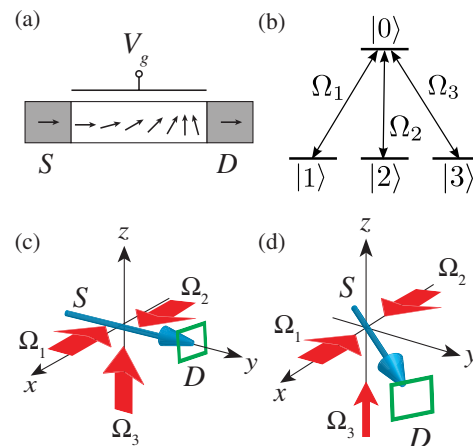


FIG. 1 (color online). (a) Schematic of a DDT. "S" and "D" are ferromagnetic source and drain electrodes. In between is a semiconducting gate region, where the spin precesses by an amount which depends periodically on the tunable gate voltage  $V_g$ . This precession results in a controllable current modulation at D. (b) A tripod scheme of atomic energy levels, coupled by laser fields with Rabi frequencies  $\Omega_j$ . (c),(d) Two alternative setups for an atomic version of the DDT. Here, the source is a state-polarized atomic beam (blue arrow labeled "S"), the gate is the intersection region of a configuration of laser beams (red arrows labeled  $\Omega_1$ ,  $\Omega_2$ , and  $\Omega_3$ ), and the drain is an atomic state analyzer (green squares).

analog of the gate voltage can be tuned by varying the relative strengths of the lasers. The drain is a state-selective atomic filter, such as a Stern-Gerlach device or radio-frequency or Raman outcoupler [18]. While the goal of this Letter is to explore the possibility of constructing the atomic analog of spintronic devices, the two dark states of the tripod atom can be considered qubit states [19–22]; in this context the atomic DDT represents a single-qubit phase gate for a dilute atomic beam. In contrast to typical single-qubit gates, this setup does not involve time-dependent pulses, and the amount of the qubit rotation within the gate region is independent of the atom's velocity, due to the geometric nature of the process.

*Tripod scheme.*—The proposed DDT implementations exploit the tripod scheme [Figs. 1(b) and 1(c)] [6–8,10,11,23], in which a four-level atom feels two counter-propagating stationary laser beams and a third orthogonal beam [14,16,17]. The lasers induce transitions between the ground states  $|j\rangle$  ( $j = 1, 2, 3$ ) and an excited state  $|0\rangle$  with spatially dependent Rabi frequencies  $\Omega_1 = |\Omega_1|e^{-i\kappa_0 x}$ ,  $\Omega_2 = |\Omega_2|e^{i\kappa_0 x}$ , and  $\Omega_3 = |\Omega_3|e^{i\kappa_0 z}$ ,  $\kappa_0$  being a wave number.

The electronic Hamiltonian of a tripod atom is, in the interaction representation and rotating wave approximation,  $\hat{H}_e = -\hbar\Omega|B\rangle\langle 0| + \text{H.c.}$ , where  $|B\rangle = (|1\rangle\Omega_1^* + |2\rangle\Omega_2^* + |3\rangle\Omega_3^*)/\Omega$  and  $\Omega^2 = |\Omega_1|^2 + |\Omega_2|^2 + |\Omega_3|^2$ .  $\hat{H}_e$  has two degenerate dark states  $|D_j\rangle$  containing no excited state contribution:  $\hat{H}_e|D_j\rangle = 0$ ,  $j = 1, 2$ . An additional pair of bright eigenstates  $|\pm\rangle = (|B\rangle \pm |0\rangle)/\sqrt{2}$  is separated from the dark states by  $\pm\hbar\Omega$ . For the light fields of interest, the dark states can be chosen as

$$|D_1\rangle = (\sin\varphi|1'\rangle - \cos\varphi|2'\rangle), \quad (1)$$

$$|D_2\rangle = \varepsilon(\cos\varphi|1'\rangle + \sin\varphi|2'\rangle) - \sqrt{1 - \varepsilon^2}|3\rangle, \quad (2)$$

with  $|1'\rangle = |1\rangle e^{i\kappa_0(z+x)}$  and  $|2'\rangle = |2\rangle e^{i\kappa_0(z-x)}$ , where

$$\varepsilon = |\Omega_3|/\Omega, \quad \varphi = \arctan(|\Omega_1|/|\Omega_2|) \quad (3)$$

characterize the relative intensities of the laser beams. The dark states  $|D_j\rangle \equiv |D_j(\mathbf{r})\rangle$  are position dependent due to the spatial variation of the Rabi frequencies  $\Omega_j(\mathbf{r})$ .

Let us adiabatically eliminate the bright states, so that the atom evolves within the dark-state manifold. The full atomic state vector can then be expanded as  $|\Psi(\mathbf{r}, t)\rangle = \sum_{n=1}^2 \chi_n(\mathbf{r}, t)|D_n(\mathbf{r})\rangle$ , where  $\chi_n(\mathbf{r}, t)$  describes the motion of an atom in the dark state  $|D_n(\mathbf{r})\rangle$ . The atomic center of mass motion is thus represented by a two-component wave function  $\chi = (\chi_1, \chi_2)^T$  obeying [7]

$$i\hbar \frac{\partial}{\partial t} \chi = \left[ \frac{1}{2M} (-i\hbar\nabla - \mathbf{A})^2 + U \right] \chi, \quad (4)$$

where  $\mathbf{A}$  is the effective vector potential [7,24–26] representing a  $2 \times 2$  matrix whose elements are vectors,  $\mathbf{A}_{n,m} = i\hbar \langle D_n(\mathbf{r}) | \nabla D_m(\mathbf{r}) \rangle$ . The particular light field configuration we have chosen yields

$$\mathbf{A}_{11} = -\hbar\kappa_0(\mathbf{e}_z - \cos(2\varphi)\mathbf{e}_x), \quad (5)$$

$$\mathbf{A}_{12} = -\hbar\varepsilon(\kappa_0 \sin(2\varphi)\mathbf{e}_x + i\nabla\varphi), \quad (6)$$

$$\mathbf{A}_{22} = -\hbar\kappa_0\varepsilon^2(\mathbf{e}_z + \cos(2\varphi)\mathbf{e}_x), \quad (7)$$

with  $\mathbf{e}_x$  and  $\mathbf{e}_z$  the unit Cartesian vectors. The  $2 \times 2$  matrix  $U$  with elements  $U_{nm} = (\hbar^2/2M)\langle D_n(\mathbf{r}) | \nabla B(\mathbf{r}) \rangle \times \langle B(\mathbf{r}) | \nabla D_m(\mathbf{r}) \rangle$  is an effective scalar potential; both  $\mathbf{A}$  and  $U$  arise due to the spatial dependence of the atomic dark states.

Suppose the incident atom has a velocity  $\mathbf{v}$  much greater than the recoil velocity  $v_{\text{rec}} = \hbar\kappa_0/M \approx 0.5$  cm/s for  $^{87}\text{Rb}$ . In this limit, the laser beams do not significantly change the atom's velocity, permitting a simplified semiclassical approach with no reflected waves. We apply a gauge transformation  $\chi(\mathbf{r}, t) = e^{iM\mathbf{v}\cdot\mathbf{r}/\hbar - iMv^2t/2\hbar} \tilde{\chi}(\mathbf{r}, t)$ , implying transition to a reference frame moving with velocity  $\mathbf{v}$ , where the two-component envelope function  $\tilde{\chi}$  varies slowly with  $\mathbf{r}$  over the atom's wavelength  $\lambda = h/(Mv)$ . Keeping only terms containing  $\mathbf{v}$  (or its time derivatives), we arrive at the following approximate equation for  $\tilde{\chi}$ :

$$i\hbar(\partial/\partial t + \mathbf{v}\cdot\nabla)\tilde{\chi}(\mathbf{r}, t) = -\mathbf{v}\cdot\mathbf{A}(\mathbf{r})\tilde{\chi}(\mathbf{r}, t). \quad (8)$$

As the omitted scalar potential  $U$  and the  $A^2$  term are of the order of the recoil energy  $\hbar\omega_{\text{rec}} = \hbar^2\kappa_0^2/2M \ll Mv^2/2$ , the fast moving atoms will not feel these potentials. For incident velocities  $v$  of the order of  $v_{\text{rec}}$  or smaller, the atomic motion will undergo a *Zitterbewegung* [15,27] which is beyond the scope of the present study. While the atoms must move much faster than the recoil velocity, they should also be slow enough to avoid coupling to the bright states. We provide a quantitative analysis of these limitations near the end of the Letter.

In both of the DDT schemes to be presented, the operator  $\mathbf{v}\cdot\mathbf{A}$  commutes with itself at different times. Going to a moving frame of reference  $\mathbf{r}' = \mathbf{r} - \mathbf{v}t$ , we can thus relate the wave function  $\tilde{\chi}$  at time  $t = t_f$  to the wave function at a previous time  $t = t_i$  through

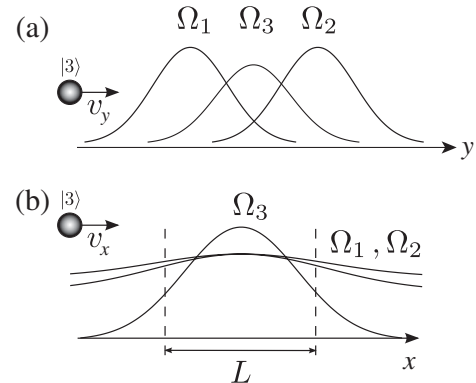


FIG. 2. Schematics of the first (a) and second (b) setups for an atomic transistor: The atom, along its trajectories [shown in Figs. 1(c) and 1(d)] sees the above profile of laser fields.

$$\tilde{\chi}(\mathbf{r}', t_f) = \exp(i\Theta)\tilde{\chi}(\mathbf{r}', t_i). \quad (9)$$

The  $2 \times 2$  Hermitian matrix  $\Theta = -\hbar^{-1} \int_{t_i}^{t_f} \mathbf{A}(\mathbf{r}' + \mathbf{v}t) \cdot \mathbf{v} dt$  describes the evolution of the internal state of the atom as it traverses the path from  $\mathbf{r}_i = \mathbf{r}' + \mathbf{v}t_i$  to  $\mathbf{r}_f = \mathbf{r}' + \mathbf{v}t_f$ ,

$$\Theta = -\frac{1}{\hbar} \int_{\mathbf{r}_i}^{\mathbf{r}_f} \mathbf{A}(\mathbf{r}) \cdot d\mathbf{r}. \quad (10)$$

Our subsequent analysis of the atomic dynamics will center on Eqs. (5)–(7), (9), and (10).

*Atomic analogs of the DDT.*—We first consider the setup depicted in Figs. 1(c) and 2(a). The atoms are incident along the  $y$  axis, along which laser beams 1 and 2 are relatively shifted [6,8,10,23], so that

$$A_y = \hbar\sigma_y \varepsilon(y) \partial \varphi(y) / \partial y. \quad (11)$$

Equations (10) and (11) yield

$$\Theta = \alpha \sigma_y, \quad \alpha = - \int_{y_i}^{y_f} \varepsilon(y) \frac{\partial}{\partial y} \varphi(y) dy, \quad (12)$$

where  $\alpha$  is the mixing angle,  $\sigma_y$  (or  $\sigma_x$ ) being the usual Pauli matrix. By taking the initial and final times sufficiently large, we have  $y_i \rightarrow -\infty$  and  $y_f \rightarrow +\infty$ .

As Figs. 1(c) and 2(a) show, the first laser beam dominates as the atom enters the gate region, while the second dominates as it exits the region. In between, the atom also feels the third beam. This configuration results in a gate-induced rotation of the atom's internal state by a mixing angle  $\alpha$ . Specifically, suppose the atom enters the gate region in the internal state  $|3\rangle = -|D_2(\mathbf{r}', t_i)\rangle$ , with center of mass wave function  $\Phi(\mathbf{r}')$ . The atom then exits the gate region in the rotated state

$$\tilde{\chi}(\mathbf{r}', t_f) = -\Phi(\mathbf{r}') \begin{pmatrix} \sin \alpha \\ \cos \alpha \end{pmatrix}. \quad (13)$$

Thus, the probability for the atom to emerge in the second dark state is  $\cos^2 \alpha$ . Note that the second dark state coincides with the third internal ground state upon exit:  $|D_2(\mathbf{r}', t_f)\rangle = -|3\rangle$ . This gate-controlled state rotation is an atomic analog of the action of the DDT. Define  $\eta = |\Omega_3|/|\Omega_1|$  as the relative amplitude of the third laser at the central point. The specific relation between  $\alpha$  and  $\eta$  depends on the particular choice of light field configuration and is readily derived from Eqs. (3) and (12). For arbitrary light field configurations,  $\alpha$  is a complicated space-dependent function. However, for the particular laser configuration we examine here,  $\alpha$  simplifies to a function solely depending on  $\eta$ , and  $\eta$  controls  $\alpha$ . Figure 3 shows the dependence of  $\alpha$  on  $\eta$  for Gaussian laser beams. As in the electronic DDT, the transmission coefficient  $\cos \alpha$  is independent of the velocity of the incident atoms, so that the transistor properties are robust to a spread in atomic velocities. We estimate the regime of validity of this independence near the end of the Letter.

Since  $\varepsilon(y) \leq 1$ , the mixing angle given by Eq. (12) ranges from 0 to  $\pi/2$ , and the sensitivity  $|\Delta \alpha|/|\Delta \eta|$  of

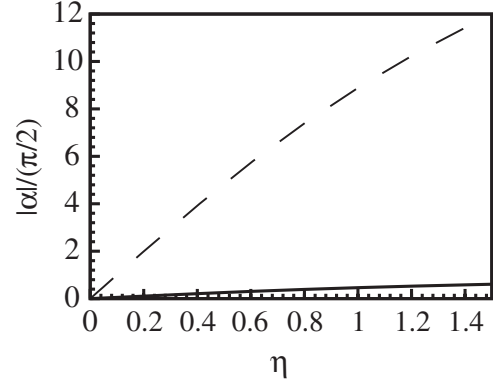


FIG. 3. The mixing angle  $\alpha$  vs the relative amplitude of the third field  $\eta$  for the first (solid line) and the second (dashed line) setups. The amplitudes of the beams are Gaussian:  $|\Omega_1| = a \exp(-(u + \delta)^2/w_1^2)$ ,  $|\Omega_2| = a \exp(-(u - \delta)^2/w_2^2)$ , and  $|\Omega_3| = a\eta \exp(-u^2/w_3^2 - \delta^2/w_1^2)$ , with  $u = y$  (first setup) or  $u = x$  (second setup). In the first setup,  $w_1 = w_2 = w_3 = \delta = 2\lambda$ , with  $\lambda = 600$  nm being the laser wave length. For the second setup, all the beams are centered at the same point ( $\delta = 0$ ) and have the widths  $w_1 = w_2 = 10w_3 = 20\lambda$ .

the DDT is on the order of unity. Small changes in the relative Rabi frequency  $\eta$  will thus lead to small changes in the mixing angle:  $|\Delta \alpha| \sim |\Delta \eta|$ . We next analyze an alternative setup which enables us to create a more sensitive DDT.

Now suppose that the first two light beams counter-propagate along the  $x$  axis with equal intensities [Fig. 1(d)], i.e.,  $\varphi = \pi/4$  in Eqs. (5)–(7) for  $\mathbf{A}$ . After the trivial gauge transformation  $\exp[i\hbar\kappa_0(1 + \varepsilon^2)z\mathbf{I}]$ , the light-induced vector potential resembles the Rashba spin-orbit coupling which is the spin rotation mechanism of the electronic DDT:

$$A_z = -\frac{\hbar\kappa_0}{2}(1 - \varepsilon^2)\sigma_z, \quad (14)$$

$$A_x = -\hbar\kappa_0\varepsilon\sigma_x, \quad A_y = 0. \quad (15)$$

The atomic beam crosses the lasers at an angle in the  $x$ - $y$  plane, with initial velocity components  $v_x \neq 0$  and  $v_y$ . Although the atomic motion in the  $y$  direction does not affect the internal state rotation ( $A_y = 0$ ), sending the beam in at an angle removes the experimental difficulty of having the atoms incident from the same direction as the laser beams. Along its trajectory, the atom feels the laser beam profile illustrated in Fig. 2(b). The evolution matrix of Eq. (10) is then

$$\Theta = \alpha \sigma_x, \quad \alpha = \kappa_0 \int_{x_i}^{x_f} \varepsilon(x) dx. \quad (16)$$

Initial and final times are taken sufficiently large that the spatial integration runs from  $x_i = -\infty$  to  $x_f = +\infty$ .

As in the previous scheme, the intensity of the third laser vanishes ( $\varepsilon \rightarrow +0$ ) outside the gate region [see Fig. 2(b)]. Only the third laser's intensity has significant spatial de-

pendence inside the gate region, the intensities of the first two lasers being nearly constant there. In both setups, the controlled state rotation arises from the spatial dependence of the beams in the gate region. In the first setup the variation is in the lasers' relative intensities. Contrastingly, in the second setup, the intensities of the first two lasers are constant in the gate region, so the controlled state rotation is driven by only the relative *phases* of the counterpropagating laser beams.

As in the previous setup, the atom enters the gate region in the internal state  $|3\rangle = -|D_2(\mathbf{r}', t_i)\rangle$  and with center of mass wave function  $\Phi(\mathbf{r}')$ . The atom exits in the rotated state

$$\tilde{\chi}(\mathbf{r}', t_f) = -\Phi(\mathbf{r}') \begin{pmatrix} i \sin \alpha \\ \cos \alpha \end{pmatrix}, \quad (17)$$

where the mixing angle  $\alpha$  is controlled by the variation of the relative intensity of the third laser beam.

To estimate the mixing angle, suppose that  $\Omega_3$ , and hence  $\varepsilon$ , do not change significantly in the gate region. Equation (16) then gives  $\alpha = \kappa_0 \bar{\varepsilon} L$ , where  $L$  [see Fig. 2(b)] is the length of the area in which the third laser has the strongest intensity. Note that the mixing angle is now proportional to  $L$ , as well as to the average strength  $\kappa_0 \bar{\varepsilon}$  of the spin-orbit coupling. This behavior is in direct analogy to the electronic DDT [1]. As in Eq. (2) of [1], the output power of the atoms in the internal state  $|3\rangle$  is  $P = \cos^2 \alpha = \cos^2(\kappa_0 \bar{\varepsilon} L)$ . Using this atomic setup,  $\alpha = \kappa_0 \bar{\varepsilon} L$  can be much larger than  $\pi/2$ , provided  $L \gg (\kappa_0 \bar{\varepsilon})^{-1}$ , as shown in Fig. 3. Small changes in the relative amplitude of the third laser  $\eta = |\Omega_3|/|\Omega_1|$  can therefore yield substantial changes in the mixing angle:  $|\Delta \alpha| \sim |\Delta \eta| \kappa_0 L$ . The sensitivity of such a DDT,  $|\Delta \alpha|/|\Delta \eta| \sim \kappa_0 L$ , can far exceed unity if  $L$  is much greater than the optical wave length  $\lambda = 2\pi/\kappa_0$ .

Let us estimate the range of atomic beam velocities for which our approximations are valid. The atom crosses the gate region in a time  $\tau = L/v$ . Because of nonadiabatic coupling to the bright states, the dark-state atoms have the finite lifetime  $\tau_D = \Omega^2/\gamma \Delta \omega^2$  [28], where  $\gamma$  is the excited state decay rate and  $\Delta \omega = v \partial \varphi / \partial y \sim v \pi / L$  (first setup), or  $\Delta \omega = v \kappa_0$  (second setup). The frequency shift  $\Delta \omega$  represents the two-photon detuning due to the finite time of the atom-light interaction (first setup) or the two-photon Doppler shift (second setup). To avoid decay, we require the beam to be in the adiabatic limit, i.e.,  $\tau/\tau_D \ll 1$ . Taking  $\Omega = 2\pi \times 10^7$  Hz [29],  $\gamma = 10^7$  s<sup>-1</sup>,  $\kappa_0 = 2\pi/\lambda$ ,  $\lambda = 600$  nm, and  $L = 4\lambda$ , we require atomic velocities  $v \ll 100$  m/s for the first setup and  $v \ll 1$  m/s for the second setup. The increased sensitivity in the second scheme thus comes at the expense of increased nonadiabatic losses.

Ultracold atoms are highly tunable and controllable, and can thus serve as quantum simulators for a variety of other systems, including systems which have yet to be experimentally accessed in their original manifestations. In this

Letter, we have identified an atomic analog of one such system, the spin field-effect transistor. Our atomic transistors, like their electronic counterpart, provide controllable state manipulation that is relatively insensitive to the thermal spread of beam velocities. The devices we have proposed are based on the familiar tripod STIRAP configuration, and appear to be feasible within current experimental procedures.

This work was partially supported by the National Science Foundation under the Physics Frontier Center grant PHY-0822671.

- 
- [1] S. Datta and B. Das, Appl. Phys. Lett. **56**, 665 (1990).
  - [2] I. Zutic, J. Fabian, and S. Das Sarma, Rev. Mod. Phys. **76**, 323 (2004).
  - [3] A. Ruschhaupt, J. G. Muga, and M. G. Raizen, J. Phys. B **39**, L133 (2006).
  - [4] B. T. Seaman, M. Krämer, D. Z. Anderson, and M. J. Holland, Phys. Rev. A **75**, 023615 (2007).
  - [5] J. J. Thorn, E. A. Schoene, T. Li, and D. A. Steck, Phys. Rev. Lett. **100**, 240407 (2008).
  - [6] R. G. Unanyan, M. Fleischhauer, B. W. Shore, and K. Bergmann, Opt. Commun. **155**, 144 (1998).
  - [7] J. Ruseckas, G. Juzeliūnas, P. Öhberg, and M. Fleischhauer, Phys. Rev. Lett. **95**, 010404 (2005).
  - [8] G. Juzeliūnas, J. Ruseckas, P. Öhberg, and M. Fleischhauer, Lithuanian J. Phys. **47**, 351 (2007).
  - [9] Y.-J. Lin *et al.*, arXiv:0809.2976.
  - [10] H. Theuer *et al.*, Opt. Express **4**, 77 (1999).
  - [11] F. Vewinger *et al.*, Phys. Rev. Lett. **91**, 213001 (2003).
  - [12] E. I. Rashba, Sov. Phys. Solid State **2**, 1224 (1960).
  - [13] T. D. Stanescu, C. Zhang, and V. Galitski, Phys. Rev. Lett. **99**, 110403 (2007).
  - [14] A. Jacob, P. Öhberg, G. Juzeliūnas, and L. Santos, Appl. Phys. B **89**, 439 (2007).
  - [15] J. Y. Vaishnav and C. W. Clark, Phys. Rev. Lett. **100**, 153002 (2008).
  - [16] G. Juzeliūnas *et al.*, Phys. Rev. A **77**, 011802(R) (2008).
  - [17] G. Juzeliūnas *et al.*, Phys. Rev. Lett. **100**, 200405 (2008).
  - [18] M. Edwards *et al.*, J. Phys. B **32**, 2935 (1999).
  - [19] L. M. Duan, J. I. Cirac, and P. Zoller, Science **292**, 1695 (2001).
  - [20] Z. Kis and F. Renzoni, Phys. Rev. A **65**, 032318 (2002).
  - [21] R. G. Unanyan and M. Fleischhauer, Phys. Rev. A **69**, 050302(R) (2004).
  - [22] S. Rebić *et al.*, Phys. Rev. A **70**, 032317 (2004).
  - [23] R. G. Unanyan, B. W. Shore, and K. Bergmann, Phys. Rev. A **59**, 2910 (1999).
  - [24] M. V. Berry, Proc. R. Soc. A **392**, 45 (1984).
  - [25] F. Wilczek and A. Zee, Phys. Rev. Lett. **52**, 2111 (1984).
  - [26] C. A. Mead, Rev. Mod. Phys. **64**, 51 (1992).
  - [27] M. Merkl, F. E. Zimmer, G. Juzeliūnas, and P. Öhberg, Europhys. Lett. **83**, 54002 (2008).
  - [28] G. Juzeliūnas, J. Ruseckas, P. Öhberg, and M. Fleischhauer, Phys. Rev. A **73**, 025602 (2006).
  - [29] L. Hau, S. E. Harris, Z. Dutton, and C. Behrooz, Nature (London) **397**, 594 (1999).